



The University of Bradford Institutional Repository

<http://bradscholars.brad.ac.uk>

This work is made available online in accordance with publisher policies. Please refer to the repository record for this item and our Policy Document available from the repository home page for further information.

To see the final version of this work please visit the publisher's website. Available access to the published online version may require a subscription.

Link to publisher's version: <http://dx.doi.org/10.1016/j.ijpharm.2015.07.025>

Citation: Kelly AL, Halsey SA, Bottom RA, Korde S, Gough T and Paradkar A (2015) A novel transfectance near infrared spectroscopy technique for monitoring hot melt extrusion. *International Journal of Pharmaceutics*, 496 (1):117–123.

Copyright statement: © 2015 Elsevier. Reproduced in accordance with the publisher's self-archiving policy. This manuscript version is made available under the CC-BY-NC-ND 4.0 license <http://creativecommons.org/licenses/by-nc-nd/4.0/>

1
2
3 A Novel Transflectance Near Infrared Spectroscopy Technique for Monitoring
4 Hot Melt Extrusion

5
6 A L Kelly^{1*}, S A Halsey², R A Bottom², S Korde¹, T Gough¹, A Paradkar¹
7

8
9 ¹ Centre for Pharmaceutical Engineering Science, University of Bradford BD7 1DP, UK

10 ² Thermo Fisher Scientific, Stafford House, Boundary Way, Hemel Hempstead HP2 7GE,
11 UK
12
13
14
15
16
17
18
19
20
21
22
23
24
25
26

27 Corresponding Author:

28
29 Dr Adrian Kelly

30 Centre for Pharmaceutical Engineering Science,

31 University of Bradford, Bradford, BD7 1DP, UK

32 Tel: 00 44 1274 234532

33 Email: A.L.Kelly@Bradford.ac.uk

34 **ABSTRACT**

35
36 A transfectance near infra red (NIR) spectroscopy approach has been used to simultaneously
37 measure drug and plasticiser content of polymer melts with varying opacity during hot melt
38 extrusion. A high temperature reflectance NIR probe was mounted in the extruder die directly
39 opposed to a highly reflective surface. Carbamazepine (CBZ) was used as a model drug, with
40 polyvinyl pyrrolidone-vinyl acetate co-polymer (PVP-VA) as a matrix and polyethylene
41 glycol (PEG) as a plasticiser. The opacity of the molten extrudate varied from transparent at
42 low CBZ loading to opaque at high CBZ loading. Particulate amorphous API and voids
43 formed around these particles were found to cause the opacity. The extrusion process was
44 monitored in real time using transfectance NIR; calibration and validation runs were
45 performed using a wide range of drug and plasticiser loadings. Once calibrated, the
46 technique was used to simultaneously track drug and plasticiser content during applied step
47 changes in feedstock material. Rheological and thermal characterisations were used to help
48 understand the morphology of extruded material. The study has shown that it is possible to
49 use a single NIR spectroscopy technique to monitor opaque and transparent melts during
50 HME, and to simultaneously monitor two distinct components within a formulation.

51
52
53 Keywords: Hot melt extrusion
54 Near infrared spectroscopy
55 Process analytical technology
56 Carbamazepine,
57 PVP-VA

60 1. INTRODUCTION

61 Hot Melt Extrusion (HME) is a continuous melt mixing process which can be used to
62 generate amorphous drug forms in order to improve solubility. Typically, Active
63 Pharmaceutical Ingredients (APIs) are dissolved or dispersed within a soluble polymer matrix
64 (Crowley et al., 2007). Such approaches can be used to improve or control drug release and
65 inhibit drug recrystallisation (Qi et al., 2008). HME generally refers to twin screw extrusion,
66 which is a highly efficient mixing process whereby the polymer and additives are gradually
67 melted by the action of rotating screws and heat transferred through the extruder barrel.
68 Typically HME renders the drug amorphous, a state which can significantly enhance both
69 drug solubility and bioavailability. The use of HME for manufacture of pharmaceuticals has
70 been widely reported including applications such as pellets (Follonier et al., 1994), sustained
71 release tablets (Tran et al., 2011; Crowley et al., 2004), implants (Bhardwaj and Blanchard,
72 1997) and transdermal films (Aitken-Nichol et al., 1996). A number of comprehensive
73 reviews of the pharmaceutical HME process are available (Crowley et al., 2007; Repka et al.,
74 2007; Repka et al., 2012).

75 During HME the API, polymer and other excipients are conveyed through a heated barrel by
76 two closely intermeshing screws. The temperatures, mixing intensity and residence time to
77 which the materials are subjected during the process can be varied by adjusting parameters
78 such as set temperature, throughput, screw rotation speed and extruder screw configuration.
79 Within the process the API and carriers experience high temperatures and levels of shear,
80 which serve to melt the polymer and dissolve or disperse the API within the matrix.
81 However, these harsh conditions can have adverse affects on many APIs, particularly those
82 with thermolabile properties. Careful choice of excipients and optimisation of processing
83 conditions are necessary in order to avoid degradation and produce a compound with the
84 desired morphology and properties.

85 HME has the advantage of being a continuous process which means that following an initial
86 start up and stabilisation period, a consistent output can be maintained indefinitely, providing
87 that the input feed of materials is correctly maintained. Continuous processes are also well
88 suited to in-line monitoring, or Process Analytical Technology (PAT). The FDA now
89 encourages process innovation in the pharmaceutical industry through better process
90 understanding achieved by adopting Quality by Design (QbD) and PAT (FDA Guidance for
91 Industry, 2004). A range of techniques have been employed to monitor hot melt extrusion,

92 with spectroscopic measurements using high temperature probes most widely used (Saerens
93 et al., 2013). Raman and near infra-red (NIR) spectroscopy techniques can provide qualitative
94 and quantitative information about chemical and physical properties (De Beer et al., 2010).
95 NIR spectroscopy is a rapid, non-destructive technique which refers to study of light
96 absorption in the NIR region between 700-2500 nm and can be applied to the HME process
97 (Wahl et al., 2013; Luypaert et al., 2007). The technique has been used to study melt
98 extrusion of metoprolol tartrate at different loadings in a polyvinyl pyrrolidone – polyvinyl
99 acetate copolymer (Saerens et al., 2012). Results demonstrated that NIR could be used to
100 monitor API concentration and polymer-drug inter-molecular interactions. NIR has also been
101 successfully used to monitor extrusion co-crystallisation (Kelly et al., 2012; Moradiya et al.,
102 2014a; Moradiya et al., 2014b). The use of Raman spectroscopy as a PAT tool for melt
103 extrusion has also been reported, during extrusion of metoprolol tartrate and Eudragit, a
104 commercial acrylic copolymer (Saerens et al., 2011). Raman and NIR spectroscopy have
105 been used as complementary techniques to during HME of metoprolol tartrate with blends of
106 polyethylene oxide and ethylene vinyl acetate (Almeida et al., 2012). Analysis of the
107 spectroscopic data provided an improved understanding of the effects of process settings on
108 the solid state of the API.

109 A limitation of NIR spectroscopy in HME applications is that molten API/polymer systems
110 can exhibit varying levels of reflectivity. Extrudates may range between clear and opaque
111 depending upon API concentration and set temperature. In such cases a single design of
112 probe type, reflectance or transmission, may not be used to collect spectra for all melt types.
113 Reflectance probes can only gather spectra from cloudy or opaque melts and transmission
114 probes are only suitable for clear melts. The aim of the current work was to apply a novel
115 transreflectance measurement technique to characterise a range of melts with varying levels of
116 reflectivity. The design of the measurement system is described and a case study used to
117 demonstrate the application of the technique to simultaneously measure two components
118 during HME.

119 **2. MATERIALS AND METHODS**

121 **2.1 Materials**

122 Carbamazepine (CBZ) was used as a model API, procured from Jai Radhe Sales India. This
123 is an anticonvulsant and mood stabilising drug which has a molecular weight of 236 g/mol

124 and a melting temperature of 190°C. Polyvinyl pyrrolidone-vinyl acetate (PVP-VA)
125 copolymer (Kollidon® VA 64) was used as a matrix polymer, supplied by BASF, Germany.
126 This has a molecular weight of 45,000 – 70,000 g/mol, a glass transition temperature (T_g) of
127 101°C and a degradation temperature of 230°C. Polyethylene glycol (PEG) PEG2000 was
128 used as a plasticiser, procured from Sigma Aldrich. This had a molecular weight of 2000
129 g/mol and a melting point of 50-53°C and was used to lower the viscosity of the materials to
130 facilitate extrusion. PEG was introduced into the formulation to enable melt extrusion at a
131 suitable temperature; CBZ alone added to PVP-VA was not found to provide sufficient levels
132 of plasticisation. Physical mixtures of polymer, API and plasticiser were accurately weighed
133 and mixed in a mortar and pestle prior to extrusion.

134 **2.2 Methods**

135 **2.2.1 Hot Melt Extrusion**

136 Extrusion was performed using a co-rotating twin screw pharmaceutical grade extruder
137 (Pharmalab, Thermo Scientific, UK) with screw diameter 16mm and a screw length to
138 diameter ratio of 40:1. The extruder barrel comprised 10 separately temperature controlled
139 zones. Material feeding was achieved using a gravimetric twin screw feeder (Mini-twin,
140 Brabender, Germany). A slit die was designed to fit onto the front of the extruder, housing
141 two sensor probes, located directly opposite each other across the melt flow, across a 1mm
142 gap (Figure 1). The transreflectance measurement geometry comprised a high temperature
143 reflectance NIR probe located in one port of the extruder die, and a stainless steel ‘blank’
144 sensor bolt with a polished tip located directly opposite the reflectance probe. This set up
145 was designed such that opaque melts could be measured directly using the conventional
146 reflectance probe whereas for transparent melts light passing through the melt would be
147 reflected from the polished surface and be collected by the reflectance probe. Photographs of
148 extrudates produced with different levels of CBZ and PEG are shown in Figure 2.

149 Physical mixtures of CBZ, PVP-VA and PEG were prepared by manually mixing the
150 constituents between the ranges of 5.0 - 27.5 weight % CBZ and 5.0 – 20.0 weight % PEG,
151 with the remainder of each composition being made up of PVP-VA. All extrusion
152 experiments were performed at the same set temperatures, with temperature being profiled
153 from 40°C at the feed end to 120°C at the extruder die as shown in table 1. Temperatures
154 were selected following a series of initial extrusion trials at different set temperatures. The
155 optimum set condition provided a good consistency of extrudate to be handled, whilst

156 generating a reasonable level of torque in the extruder drive. Blended physical mixtures were
157 fed into the extruder at 360 g/hr and the extruder was operated at a screw rotation speed of 50
158 rpm.

159

160 **2.2.2 Near Infrared Spectroscopy**

161 NIR spectroscopy was performed using an Antaris II FT-NIR spectrometer (Thermo
162 Scientific, UK). Off-line powdered ingredients were placed in clear glass vials and measured
163 in reflectance mode using an integrating sphere. In-line measurements were made with a high
164 temperature reflectance probe connected to the spectrometer using a fibre optic bundle. This
165 probe was mounted in the extruder die as described above. For both off-line and in-line
166 measurements, each sample reading averaged 32 individual spectra at a resolution of 8 cm^{-1} ,
167 scanned over the region of $4,000\text{--}10,000\text{ cm}^{-1}$. The Thermo Scientific RESULT software
168 was used to collect spectra. Off-line powder measurements were recorded singly and the in-
169 line measurements were recorded continuously at the exit die. Data collection time was
170 approximately 30 seconds per spectrum. Measured spectra were then stored for subsequent
171 analysis with Thermo Scientific TQ Analyst software.

172

173 For each extrusion experiment, NIR spectra were collected in real time until the spectra were
174 observed to stabilise. For the experimental conditions used, this took approximately 15-20
175 minutes. NIR spectra at stable conditions were then collected for a period of around 10
176 minutes before a new blend was introduced into the feeder and the process repeated. An
177 experimental design was used to minimise the correlation, 0.14, between the components. In-
178 line measurements on nineteen mixtures were used as a calibration set and four mixtures were
179 analysed as validation samples.

180 **2.2.3 Rheological Characterisation**

181 Off-line rheological characterisation was carried out using a Physica MCR 501 rotational
182 rheometer (Anton Paar, Austria) with parallel plate geometry of diameter 25mm. The gap
183 between the two plates was set to 1 mm for all tests. Frequency sweeps were performed at a
184 set temperature of 140°C and a constant strain of 3%; this value having been determined to
185 be within the linear viscoelastic range by preceding strain amplitude tests. The angular
186 frequency range tested was $0.1 - 100\text{ s}^{-1}$. Samples were prepared by mixing the desired ratio
187 of drug, polymer and plasticiser in a mortar and pestle before placing the powdered mixture

188 on to the heated lower plate of the rheometer. Approximately one minute was allowed for the
189 material to soften prior to the upper plate being lowered to the desired gap width of 1mm and
190 any excess material was removed. The effect of CBZ and PEG on the viscosity of the
191 compound was quantified by examining physical mixtures containing a range of CBZ
192 loadings between 7.5 and 20 wt% (with PEG fixed at 10 wt%) and a range of PEG loadings
193 from 2.5 – 15 wt% (with CBZ fixed at 10 wt%).

194 **2.2.4 Scanning Electron Microscopy (SEM)**

195 Extruded samples were mounted on aluminium pin-stubs (Agar Scientific, Stansted, U.K.)
196 using self adhesive carbon mounts (Agar Scientific). The mounted samples were examined
197 using FEI Quanta 400 Scanning Electron Microscope (Cambridge, U.K.) in high vacuum
198 operated at an acceleration voltage of 20 kV.

199 **2.2.5 X-ray powder diffraction (XRPD)**

200 The crystallinity of milled samples of extrudate and pure API were assessed by X-ray powder
201 diffraction (XRPD) within 24 hours of extrusion, using a Bruker D8 diffractometer
202 (wavelength of X-rays 0.154 nm Cu source, voltage 40 kV, and filament emission 40 mA).
203 Samples were scanned from 2 to 30° (2 θ) using a 0.01° step width and a 1 s time count. The
204 receiving slit was 1° and the scatter slit was 0.2°.

206 **3. RESULTS AND DISCUSSION**

207 **3.1 Rheological Characterisation**

208 Complex viscosity of physical mixtures containing varying levels of CBZ and PEG are
209 displayed in Figure 3. PEG had a significant effect on melt viscosity over the range
210 examined, with complex viscosity decreasing from 500 Pa.s at 2.5% PEG loading to 65 Pa.s
211 at 15% PEG content. CBZ was observed to have a much less significant effect on melt
212 viscosity, causing a relatively small decrease of 10% between 7.5 and 20% loading. These
213 differences in flow behaviour were apparent during the extrusion experiments, as evidenced
214 by extruder motor torque measurements shown in Figure 4. Motor torque reflects the levels
215 of energy required to turn the extruder screws at the set rotation speed; these measurements
216 were found to closely reflect the viscosity results show in Figure 3.

217

218 **3.2 Structural Characterisation**

219 X-ray diffractograms of extruded materials are compared to those of carbamazepine in
220 figures 5a and 5b. The crystalline peaks evident in CBZ were not observed in any of the
221 extruded compounds, even at a CBZ loading of 30 wt%. These results demonstrate that the
222 crystalline CBZ was converted to an amorphous form during extrusion.

223 **3.3. Morphological Characterisation**

224 Scanning electron microscopy was performed on surfaces of extrudates in an attempt to
225 understand the opaque nature of compounds with higher CBZ loadings. Figure 6 shows
226 results from the fractured cross section (a) and outer surface (b) of an extruded strand
227 containing 30% CBZ and 10% PEG. The polymer matrix (PVP-VA) being amorphous in
228 nature is predominantly transparent. However, the presence of particulates with diameters in
229 the range of 10-30 microns and a number of voids or bubbles are evident from these images.
230 It is thought that amorphous particulates of API were formed during extrusion which led in
231 some cases to voids forming around the particles. Due to the high melting temperature of the
232 API (190 °C) a solid solution could not be formed during extrusion at higher API loadings.
233 These particulates and voids explain the opaque appearance of the extrudates.

234 **3.4. Near Infra-red spectroscopy**

235 NIR spectra of the powdered feedstock materials were measured to determine the peaks of
236 interest for both the CBZ and PEG, as shown in Figure 7. NIR spectra are typically broad and
237 overlapping and are usually enhanced with a derivative mathematical treatment. A second
238 derivative treatment was applied to these spectra, as shown in Figure 8. Strong and unique
239 peaks could be seen for CBZ, but the PEG peaks were weaker and tended to overlap with the
240 other two components. The 5600-6000 cm^{-1} region showed the most promise for the PEG
241 measurement. For this reason, partial least squares (PLS) was selected for the regression
242 method as this has been shown to have the ability to extract information from convoluted
243 peaks (Faber and Kowalski, 1977).

244 Figure 9 shows the NIR spectra of some selected samples collected at the extruder exit die;
245 the samples ranged from clear to opaque. It should be noted that the 4500-4000 cm^{-1} region
246 was noisy due to energy losses along the fibre optic bundle. This region was left out of the
247 calculations during method development. This figure also shows that the baseline of the
248 spectra changed quite considerably with different sample compositions. This was due to the

249 samples having different scattering properties as samples varied widely in cloudiness.
250 However, the use of the transmittance measurement technique allowed data to be collected
251 for all sample types. During method development a derivative mathematical treatment
252 minimised the effect of the change in baseline on the final measurements. The region chosen
253 for regression was $6208\text{-}4754\text{ cm}^{-1}$ which incorporated peaks from both CBZ and PEG.

254 Figure 10 shows the change in the second derivative spectra for the CBZ concentration when
255 the PEG was held constant. Several peaks were seen to increase in accordance with the CBZ
256 concentration, the peak at 5064 cm^{-1} being particularly strong. Figure 11 shows the change in
257 second derivative spectra for the PEG concentration when the CBZ was held constant. The
258 $5600\text{-}6000\text{ cm}^{-1}$ region did exhibit some changes, but the PEG peaks were masked by the
259 other components.

260 In-line measurements were used to calibrate the NIR instrument. Three or four spectra were
261 used from each extrudate and the samples were split into calibration (66 samples) and
262 validation (12 samples) sets. The results from the PLS regression are shown in Figure 12.
263 Correlation coefficients of >0.99 were achieved between the NIR results and the weight data
264 for CBZ measurements. Four factors were used for the CBZ calibration which gave good
265 calibration (RMSEC) and validation (RMSEP) errors of 0.788% and 0.672% respectively.
266 The PEG calibration was slightly less accurate with a calibration error of 0.633% and a
267 validation error of 1.06%. The correlation coefficients dropped to 0.986 and 0.967
268 respectively. Six factors were required to achieve this calibration which was expected
269 considering the PEG peaks were much less prominent than those for CBZ.

270 These calibrations were then used to monitor an extrudate in real time for both CBZ and PEG
271 concentrations. A step change in the content of feedstock material was applied and calibrated
272 NIR signals used to dynamically track these changes at the extruder die. CBZ level was
273 changed from 22.5% to 16% and PEG loading from 9% to 11%. The concentrations of both
274 components were measured simultaneously and plotted against time, as shown in Figure 13.
275 A smooth transition can be seen from the two original concentrations to the two new
276 concentrations; demonstrating that these measurements could be used for routine quality
277 control of an extrudate. In addition, this data showed that it took approximately 15 minutes
278 for the new batch of material to fully flush the previous sample through the extruder under
279 these process conditions. However, it should be noted that these experiments were performed
280 at relatively low throughput and screw rotation speed. Typical residence times in production
281 are likely to be significantly lower.

282

283 **4. CONCLUSIONS**

284 A transmittance FT-NIR spectroscopy technique was developed for monitoring the hot melt
285 extrusion process. A slit die was designed which enabled a reflectance NIR probe to be
286 mounted directly opposite a highly polished surface, enabling measurements to be performed
287 in both transmittance and reflectance modes. The technique was successfully applied to
288 extrusion of carbamazepine in a polyvinyl pyrrolidone-vinyl acetate copolymer matrix with
289 polyethylene glycol used as a plasticiser. At low API content the melt was transparent
290 whereas at higher loadings it became opaque due to the presence of particulate API and voids
291 which formed around these particles. Calibration of the NIR technique was performed using
292 a wide range of API and plasticiser loadings. The calibrated technique was used to
293 simultaneously monitor the loading of both API and plasticiser in real time, across
294 transparent and opaque melt regions.

295

296 **Acknowledgement**

297 The authors gratefully acknowledge BASF SE for supply of polymer used in the study.

298

299 **REFERENCES**

- 300 1. Aitken-Nichol, C., Zhang, F., McGinity, J.W., 1996. Hot melt extrusion of acrylic
301 films. *Pharm. Res.* 13, 804–808.
- 302 2. Almeida, A., Saerens, L., De Beer, T., Remon, J.P., Vervaet, C., 2012. Upscaling and
303 in-line process monitoring via spectroscopic techniques of ethylene vinyl acetate hot-
304 melt extruded formulations, *Int. J. Pharm.* 439, 223-229.
- 305 3. Bhardwaj, R., Blanchard, J., 1997. In vitro evaluation of poly(D,L-lactide-co-
306 glycolide) polymer-based implants containing the alpha-melanocyte stimulating
307 hormone analog, melanotan-I. *J. Control. Release.* 45, 49–55.
- 308 4. Crowley, M.M., Schroeder, B., Fredersdorf, A., Obara, S., Talarico, M., Kucera, S.,
309 2004. Physicochemical properties and mechanism of drug release from ethyl
310 cellulose matrix tablets prepared by direct compression and hot melt extrusion. *Int. J.*
311 *Pharm.* 271, 77–84.

- 312 5. Crowley M.M., Zhang, F., Repka, M.A., Thumma, S., Upadhye, S.B., Battu, S.K.,
313 McGinity, J.W., Martin, C.C., 2007. Pharmaceutical applications of hot-melt
314 extrusion: Part I, *Drug Dev. Ind. Pharm.* 33, 909-926.
- 315 6. De Beer, T., Burggraeve, A., Fonteyne, M., Saerens, L., Remon, J.P., Vervaet, C.,
316 2010. Near infra red and Raman spectroscopy for the in-process monitoring of
317 pharmaceutical production processes. *Int. J. Pharm.* 417, 32–47.
- 318 7. Faber, K., and Kowalski, B.R., 1997. Propagation of measurement errors for the
319 validation of predictions obtained by principal component regression and partial least
320 squares, *J. Chemometr.* 11, 181-238.
- 321 8. Follonier, N., Doelker, E., Cole, E.T., 1994. Evaluation of hot-melt extrusion as a new
322 technique for the production of polymer-based pellets for sustained release capsules
323 containing high loadings of freely soluble drugs, *Drug Dev. Ind. Pharm.* 20, 1323–
324 1339.
- 325 9. Food and Drug Administration, 2004. Process Analytical Technology Initiative,
326 Guidance for Industry PAT – A Framework for Innovative Pharmaceutical
327 Development, Manufacturing and Quality Assurance.
- 328 10. Kelly, A.L., Gough, T., Dhumal, R.S., Halsey, S.A., Paradkar, A., 2012. Monitoring
329 Ibuprofen-Nicotinamide Cocrystal Formation during Solvent Free Continuous
330 Cocrystallization (SFCC) using Near Infrared Spectroscopy as a PAT tool, *Int. J.*
331 *Pharm.* 426, 15-20.
- 332 11. Luypaert, J., Massart, D.S., Vander Heyden, Y., 2007. Near-infrared spectroscopy
333 applications in pharmaceutical analysis, *Talanta.* 72, 865–883.
- 334 12. Moradiya, H., Islam, M.T., Woollam, G.R., Slipper, I.J., Halsey, S., Snowden, M.J.,
335 Douroumis, D., 2014a. Continuous cocrystallization for dissolution rate optimization
336 of a poorly water-soluble drug, *Crystal Growth & Design*, 14, 189-198.
- 337 13. Moradiya, H.G., Islam, M.T., Halsey, S., Maniruzzaman, M., Chowdhry, B.Z.,
338 Snowden, M.J., Douroumis, D., 2014b. Continuous cocrystallisation of
339 carbamazepine and trans-cinnamic acid via melt extrusion processing,
340 *CrystEngComm.* 16, 3573-3583.
- 341 14. Repka, M.A., Battu, S.K., Upadhye, S.B., Thumma, S., Crowley, M.M., Zhang, F.,
342 Martin, C.C., McGinity, J.W., 2007. Pharmaceutical applications of hot-melt
343 extrusion: Part II, *Drug Dev. Ind. Pharm.* 33, 1043–1057.
- 344 15. Repka, M.A., Shah, S., Lu, J., Maddineni, S., Morott, J., Patwardhan, K., Mohammed,
345 N.N., 2012. Melt extrusion: process to product, *Expert Opin. Drug Deliv.*, 9 105-125.

- 346 16. Saerens, L., Dierickx, L., Lenain, B., Vervaet, C., Remon, J.P., De Beer, T., 2011.
347 Raman spectroscopy for the in-line polymer–drug quantification and solid state
348 characterization during a pharmaceutical hot-melt extrusion process. *Eur. J. Pharm.*
349 *Biopharm.* 77, 158–163.
- 350 17. Saerens, L., Dierickx, L., Quinten, T., Adriaensens, P., Carleer, R., Vervaet, C.,
351 Remon, J.P., 2012. In-line NIR spectroscopy for the understanding of polymer–drug
352 interaction during pharmaceutical hot-melt extrusion. *Eur. J. Pharm. Biopharm.* 81,
353 230–237.
- 354 18. Saerens, L., Vervaet, C., Remon, J.P., De Beer, T., 2013. Process monitoring and
355 visualization solutions for hot-melt extrusion: a review, *J. Pharm. Pharmacol.* 66,
356 180-203.
- 357 19. Tran, P.H-L., Tran, T.T-D, Park, J.B., Lee, B.J., 2011. Controlled Release Systems
358 Containing Solid Dispersions: Strategies and Mechanisms, *Pharm. Res.* 28, 2353-
359 2378.
- 360 20. Qi, S., Gryczke, A., Belton, P., Craig, D.Q.M., 2008. Characterisation of solid
361 dispersions of paracetamol and EUDRAGIT prepared by hot-melt extrusion using
362 thermal, microthermal and spectroscopic analysis, *Int. J. Pharm.* 354, 158-167.
- 363 21. Wahl, P.R., Treffer, D., Mohr, S., Roblegg, E., Koscher, G., Khinast, J.G., Inline
364 monitoring and a PAT strategy for pharmaceutical hot melt extrusion, *Int. J. Pharm.*,
365 2013, 455, 159-168.
- 366

367

368 Table I: Temperature profiles across the different zones of the extruder barrel (°C)

369

Zone 10	Zone 9	Zone 8	Zone 7	Zone 6	Zone 5	Zone 4	Zone 3	Zone 2	Zone 1
120	120	120	120	120	120	120	70	50	40

370

371

372 Table II: Formulation of batches used for PLS model calibration

373

CBZ (%)	PEG (%)	PVP-VA (%)
5	10	85
6	14	80
7.5	12.5	80
8	7	85
10	10	80
11	13	76
12.5	7.5	80
15	10	75
14	8	78
18	12	70
20	10	70
20	5	75
20	15	65
20	20	60
20	7.5	72.5
21	18	61
25	10	65
27.5	17.5	55
30	10	60

374

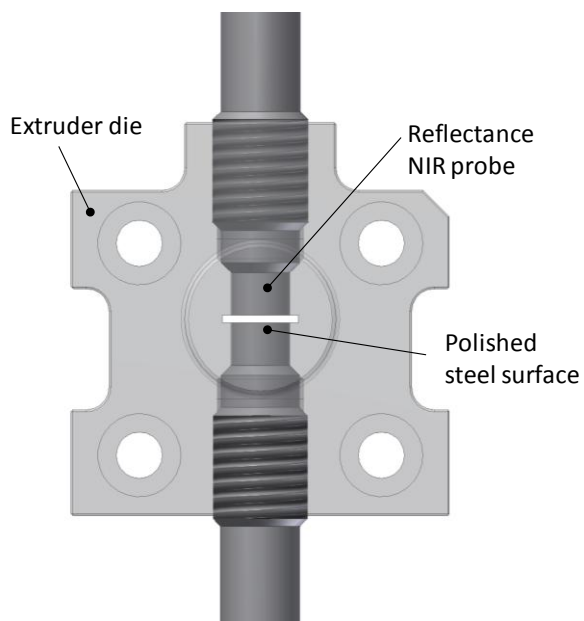
375

376 Table III: Formulation of batches used for PLS model validation

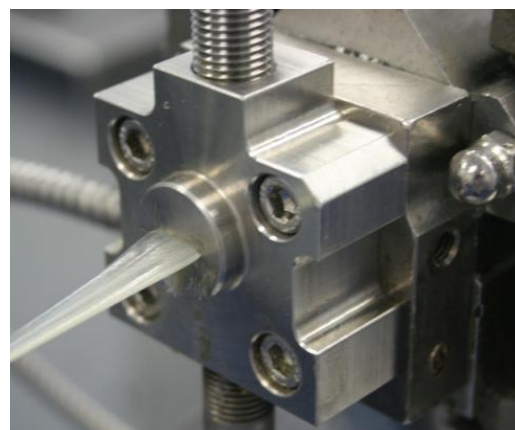
377

CBZ (%)	PEG (%)	PVP-VA (%)
9	16	75
16	11	73
22.5	9	68.5
24	19	57

378



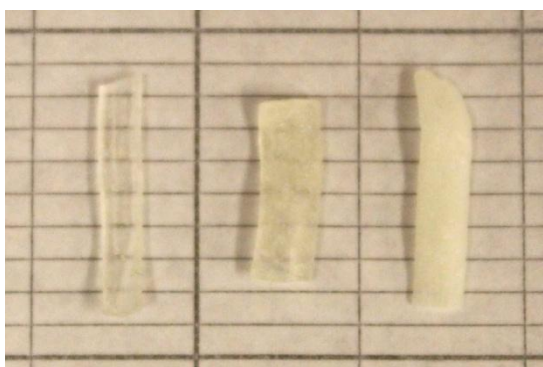
a) Model showing sensor location related to flowpath



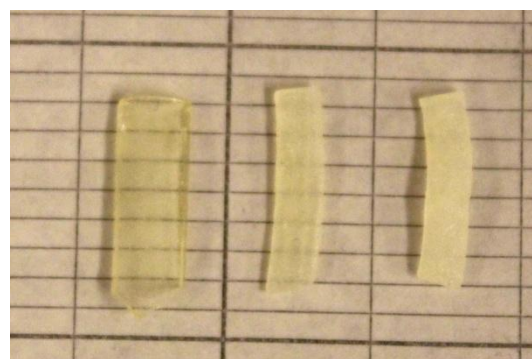
b) Photograph of die during extrusion

379
380
381

Figure 1 Pharmalab extruder die designed to accommodate two opposing sensor ports across a 1mm flow path



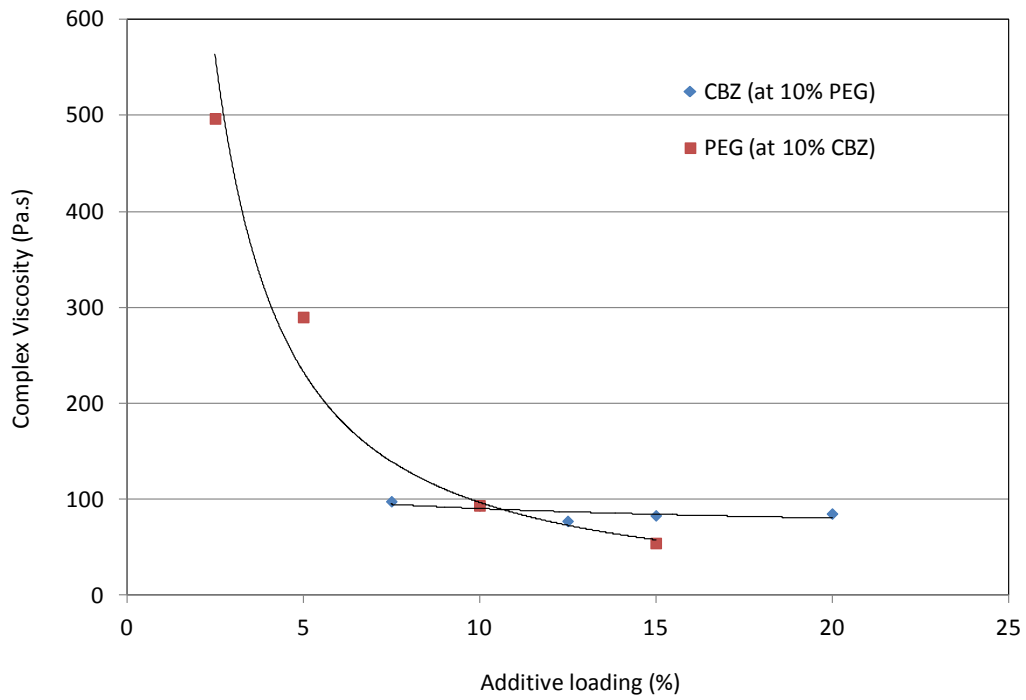
(a) 5, 15, 30% CBZ at 10% PEG



(b) 5, 15, 20% PEG at 20% CBZ

Figure 2 HME extrudate showing variation in opacity

382



383

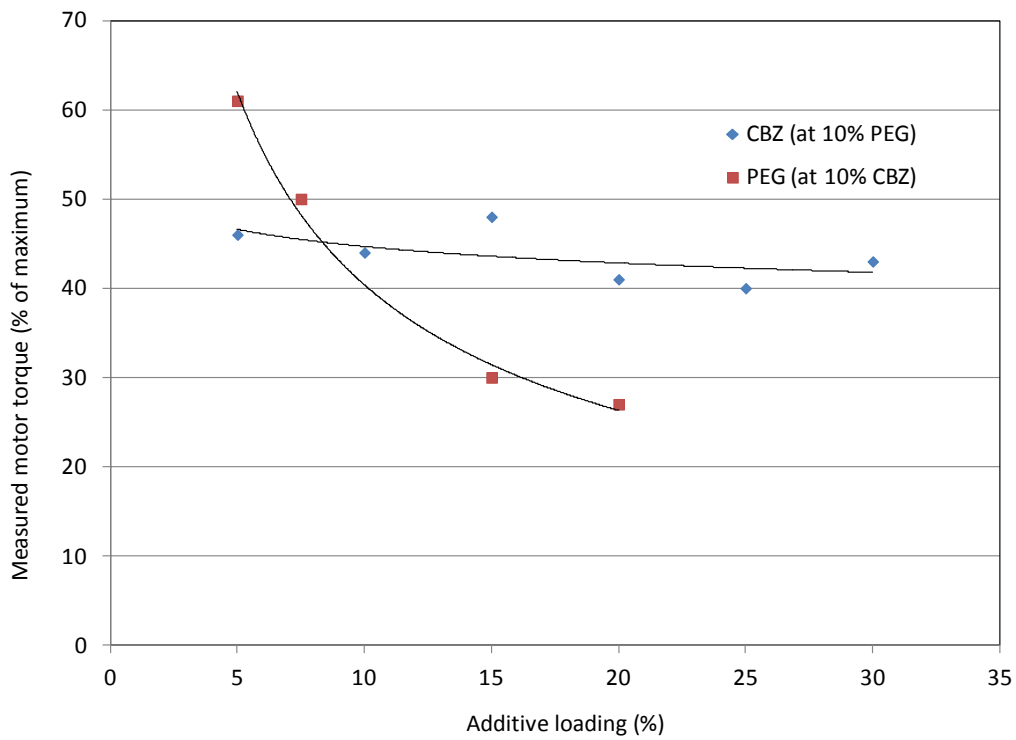
384

Figure 3 Complex viscosity of physical mixtures measured at $1s^{-1}$ showing the effect of carbamazepine and PEG loading

385

386

387



388

389

390

Figure 4 Measured extruder motor torque showing the effect of carbamazepine and PEG loading

391

392
393

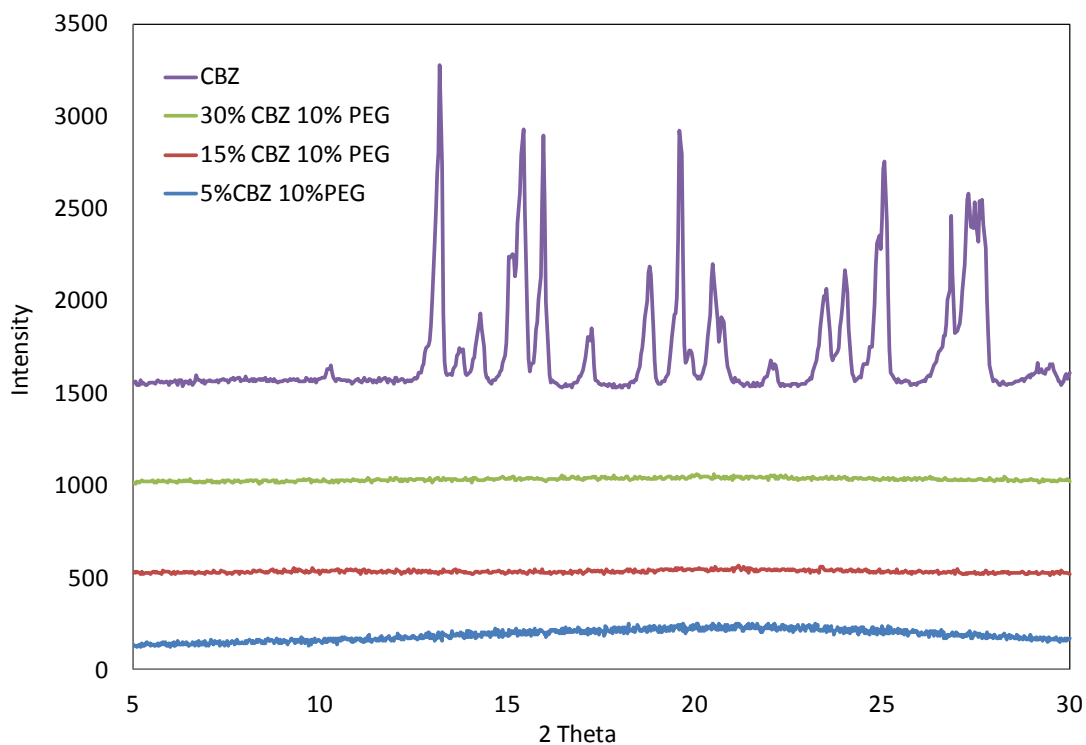


Figure 5a XRD results showing the effect of CBZ content

394
395
396
397

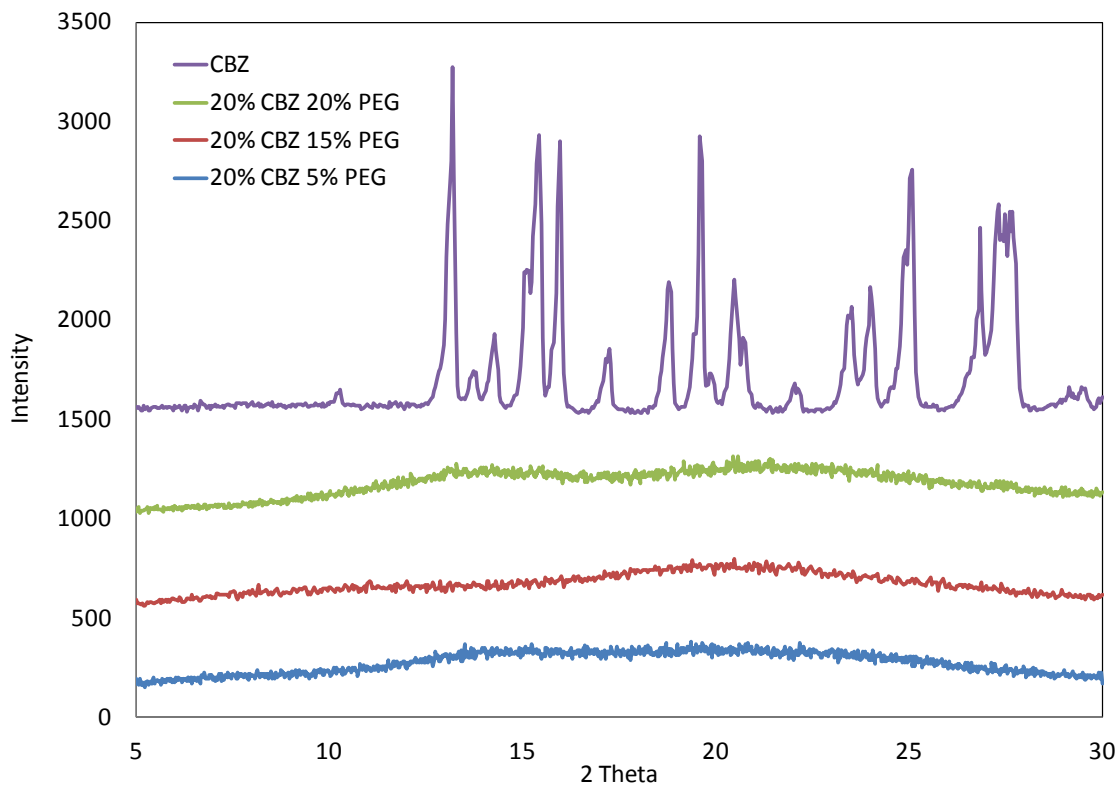
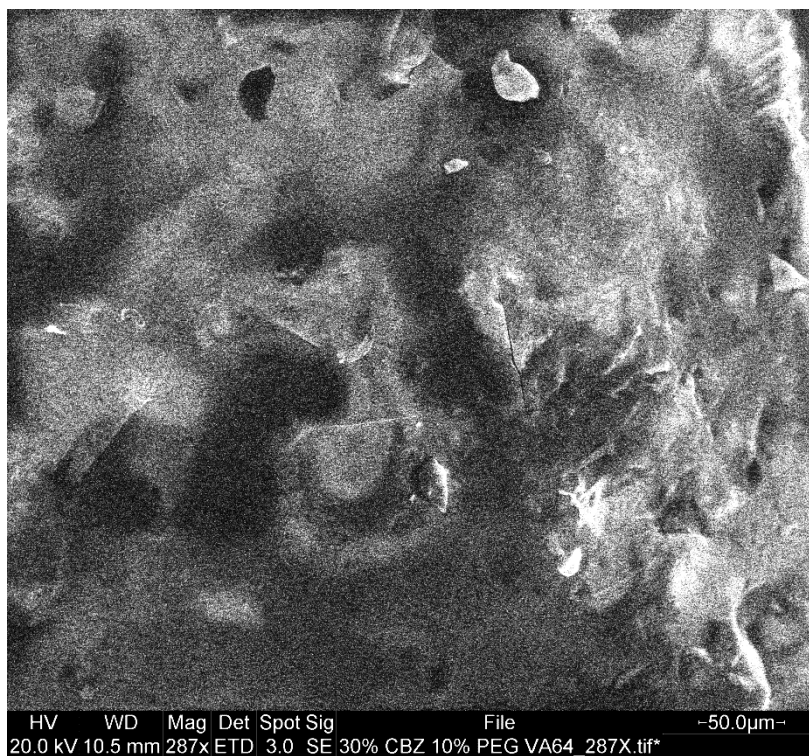


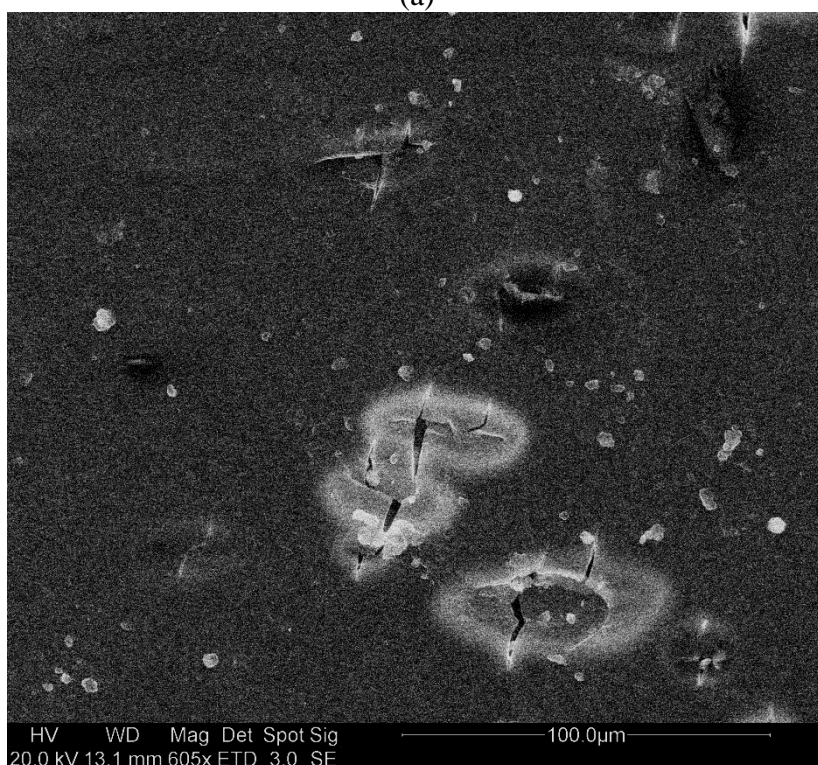
Figure 5b XRD results showing the effect of PEG content

398
399
400

401
402
403



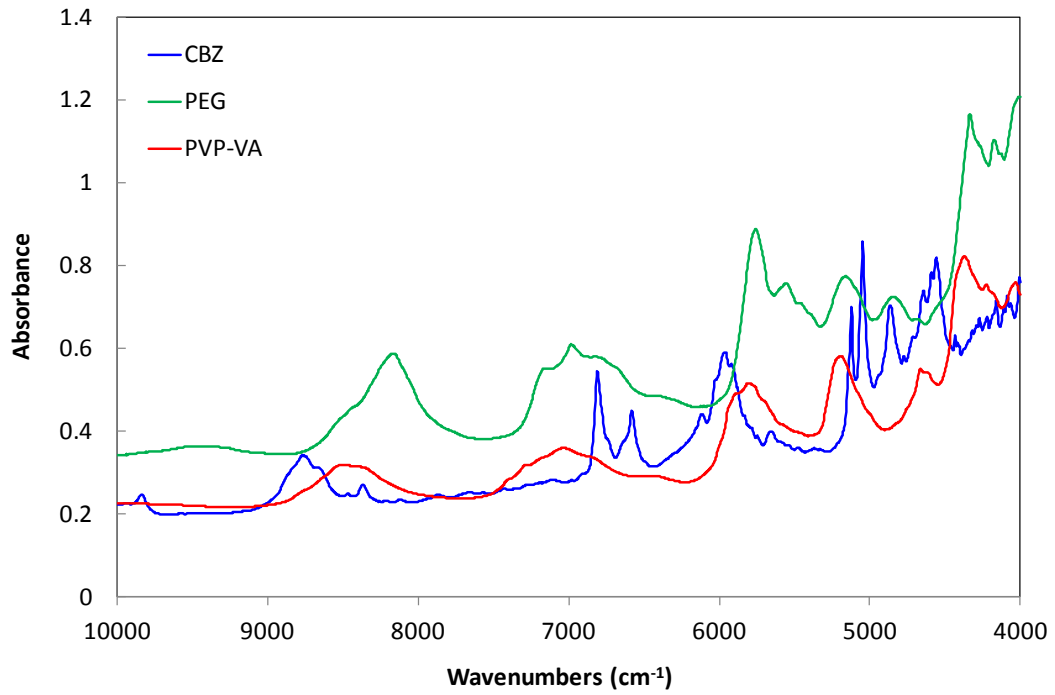
(a)



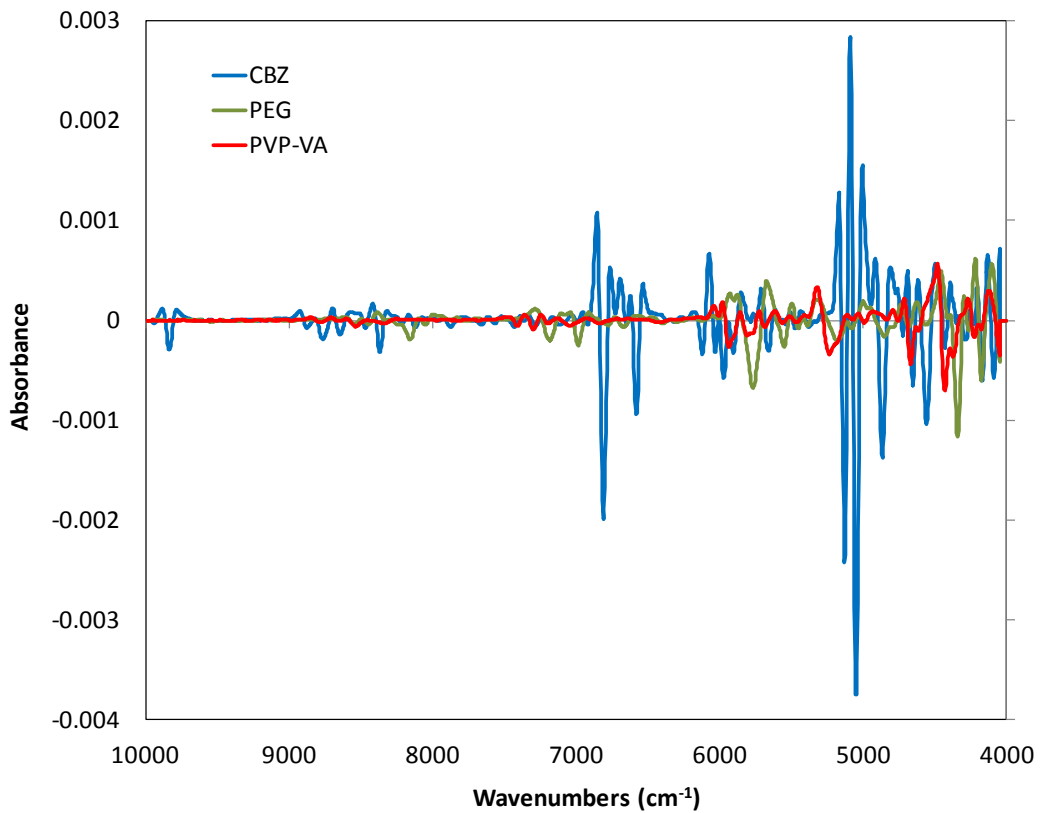
(b)

404
405
406

Figure 6 SEM images of extrudate surfaces for 30% CBZ, 10% PEG;
a) fracture surface, b) top surface of extrudate



407
408
409
Fig. 7 Off-line FT-NIR spectra of pure components



410
411
412
413
Fig. 8 Off-line second derivative spectra of pure components

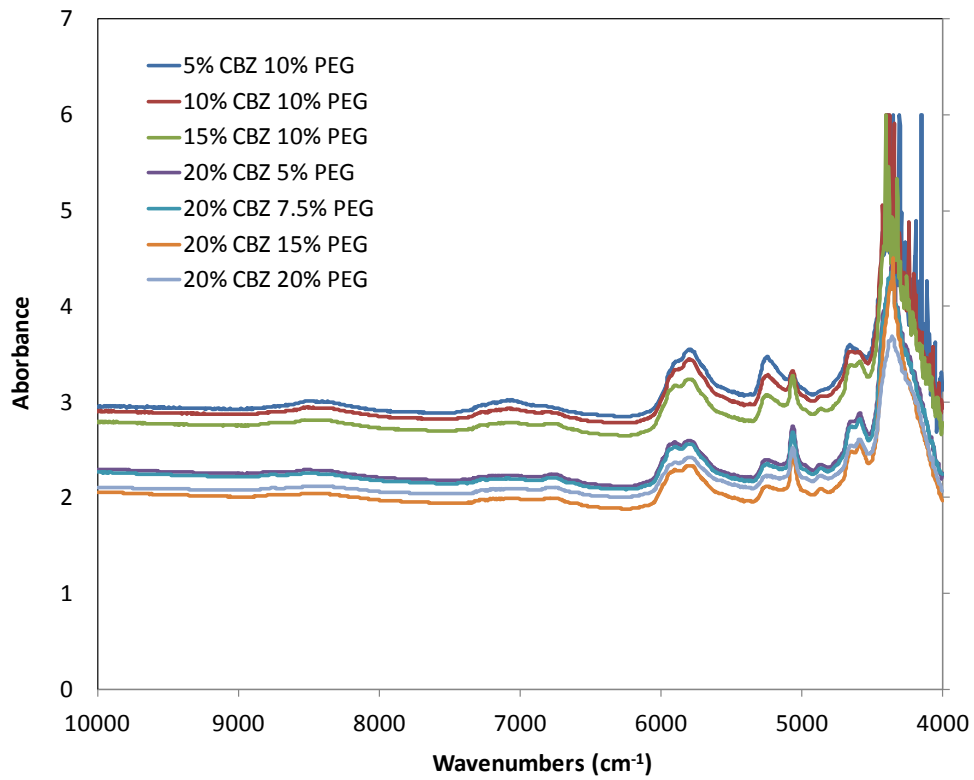


Fig. 9 In-line FT-NIR spectra of extrudates at the die exit

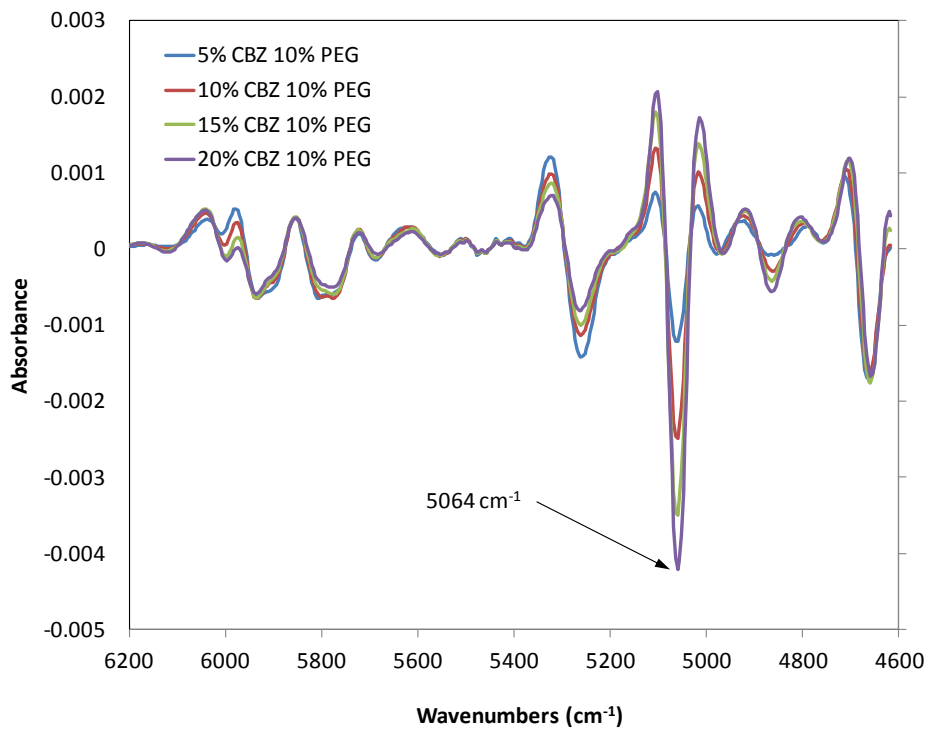
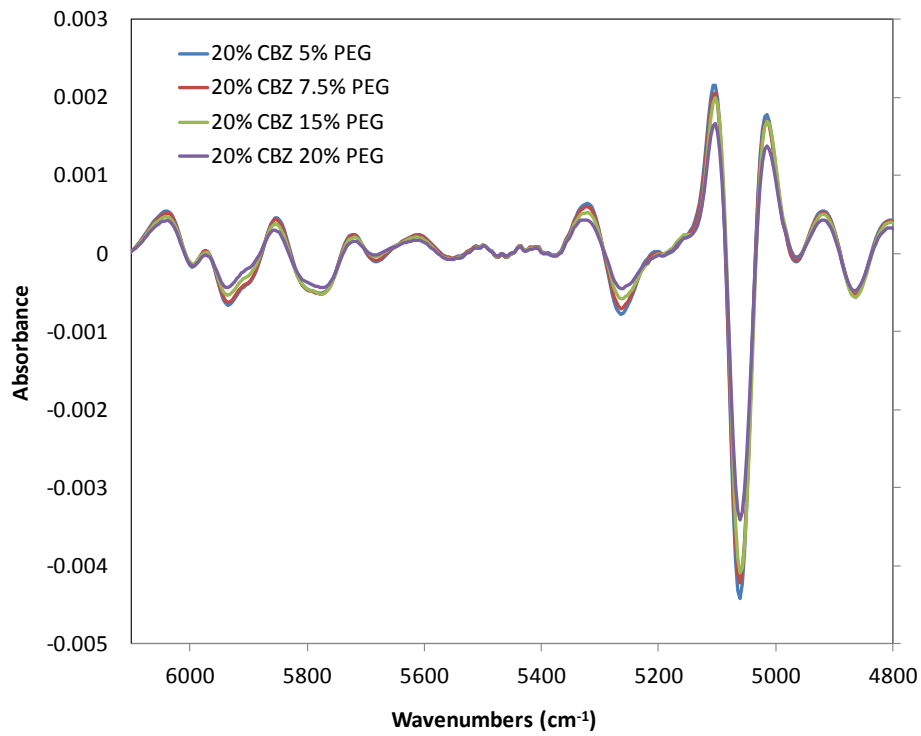


Fig. 10 In-line second derivative spectra extrudates showing CBZ concentration changes, PEG held constant at 10% by weight

421



422

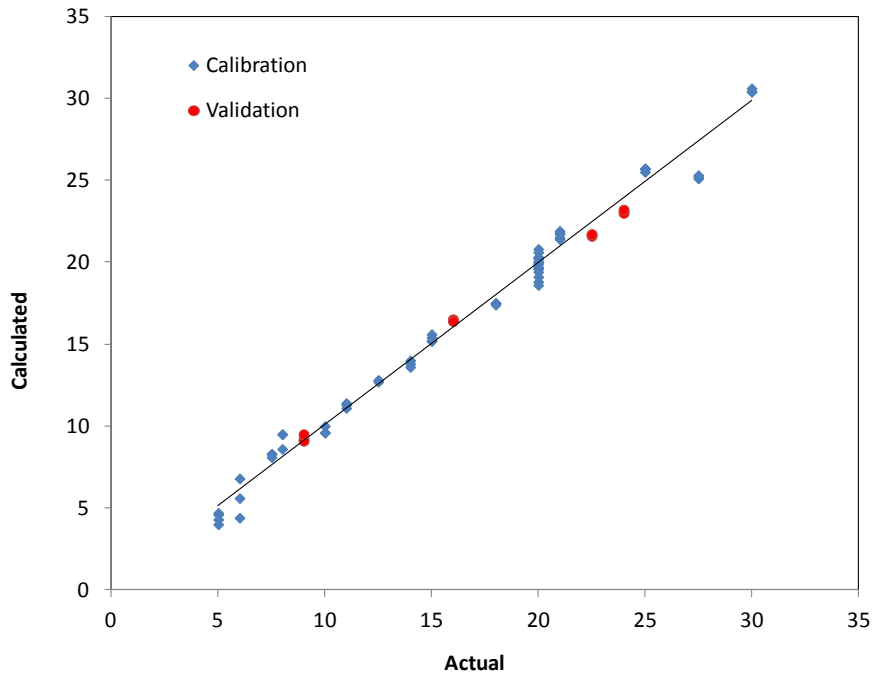
423

424

Fig. 11 In-line second derivative spectra extrudates showing PEG concentration changes, CBZ held constant at 20% by weight

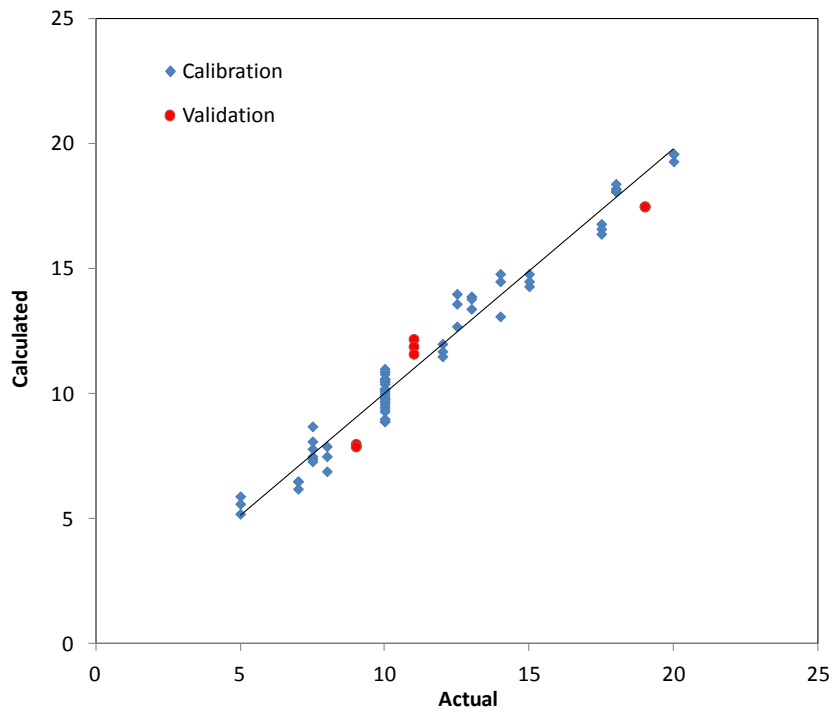
425

426



427
428
429
430

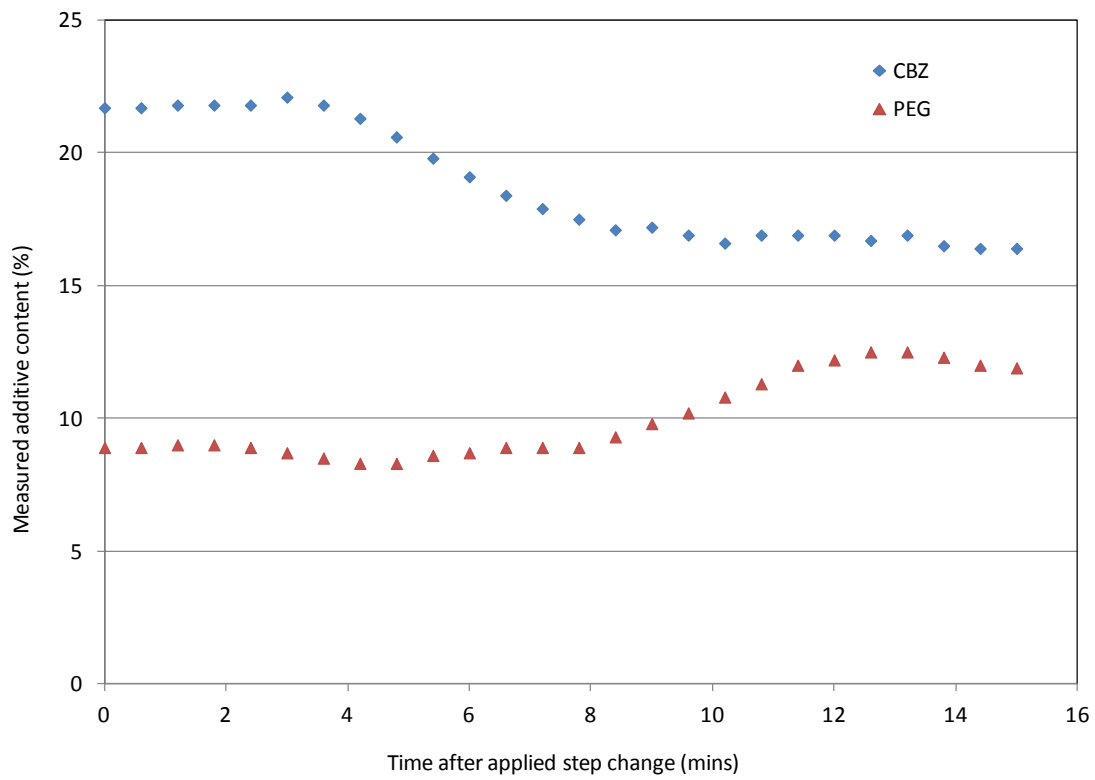
Fig. 12a PLS regression results for CBZ



431
432
433
434

Fig. 12b PLS regression results for PEG

435



436

437

438

439 Fig. 13 Plot of CBZ and PEG concentrations measured in real time following an imposed step
440 change in feedstock from 22.5% to 16% CBZ and 9% to 11% PEG

441